Scintillation Crystal Design Features for a Miniature Gamma Ray Camera

Andrew P. Dhanasopon, Craig S. Levin, *Member, IEEE,* Angela M. K. Foudray, *Student Member, IEEE,* Peter D. Olcott, Jonathon A. Talcott, *Student Member, IEEE,* and Frezghi Habte, *Member, IEEE*

***Abstract*—We are developing a miniature scintillation camera with a 5 cm x 5 cm field-of-view (FOV) to aid in surgical staging of cancer. In this paper we report on certain interesting design aspects of the scintillation crystal array. We investigated different types of crystal materials through simulations and measurements. Lutetium Oxyorthosilicate (LSO), which is ordinarily used in PET, has appealing properties for detecting 140keV photons, such as requiring only 3 mm of thickness for 95% detection efficiency at 140 keV. This small thickness is appealing for high light collection efficiency, narrow light distribution, and minimizing the LSO volume in order to reduce intrinsic background events produced by ^{176}Lu (2.6% abundance). We studied both discrete and sheet crystals and determined that discrete crystal arrays have the advantage of increased spatial linearity and dynamic range compared to crystal sheets. For optimizing sensitivity and spatial resolution, we investigated several crystal array parameters including ground crystal pixels packed tightly together without internal reflectors and without optical coupling grease. This design focuses the light, but also allows adequate light sharing for positioning with the Position Sensitive Photomultiplier Tube (PSPMT) that we are using.**

I. Introduction

Detection and localization of the closest, or "sentinel", lymph node to a primary tumor is important for the staging of cancer, because it avoids unnecessary dissection of the lymphatic system. Presently, ^{99m}Tc-Sulfur Colloid is used for the detection of the sentinel lymph nodes before surgery through lymphoscintigraphy using a standard gamma ray camera, and during surgery using a non-imaging radiation detector. Standard scintillation cameras used today for pre-surgical planning are typically not mobile and are too large to bring into a surgical suite [1]. For surgical staging, a small scintillation camera would be useful in certain situations in which the sentinel node cannot be located with a simple gamma radiation probe and/or blue dye.

Manuscript received October 31, 2003. This work was supported by the National Institutes of Health under Grant No. EB 003283-01 from the National Institute of Biomedical Imaging and Bioengineering (NIBIB) and Grant No. CA98691-01 from the National Cancer Institute (NCI).

Authors are with the VA Medical Center and the University of California San Diego School of Medicine, Department of Radiology, San Diego, CA 92161 USA (telephone: 858-552-7511, e-mail: clevin@ucsd.edu).

We are developing a miniature scintillation camera with a 5 cm x 5 cm field-of-view (FOV) that will use a Cesium doped Lutetium Oxyorthosilicate (LSO:Ce) scintillation crystal array to aid in the surgical staging of cancer. We performed both simulations and experiments to guide the choice of crystal material and crystal array parameters, which includes studies of light collection and light distribution. We report on the interesting design features of the LSO crystal array for our camera.

II. Materials and Methods

A. DETECT2000 for Simulation Studies

Monte Carlo simulations for determining both the optimal crystal material and the design features of the crystal array were performed using DETECT2000 and BUILDER Version 6 [2-5].

DETECT2000 models the behavior of optical systems by isotropically generating individual scintillation photons in specified portions of the scintillator. The simulation follows each photon in its passage through the various components and interactions with surfaces, and records the fate (absorption, escape, or detection) of each. Random samplings are made to determine if the photon is bulk absorbed, scattered, or wavelength shifted over this path. If none of these processes occur, the optical properties of the next surface determine whether the photon is reflected, refracted, detected, or absorbed. This process is then repeated for all subsequent paths in the history. Data of the fate of each photon is tabulated for all photons generated.

The program uses initial definition statements to specify the optical properties of all materials and surface finishes used in the simulation. Components are then built out of these materials and finishes. The optical behavior of each surface is chosen by selecting one of a set of previously defined surface finishes. Surfaces may either be external (assumed to be an interface with a vacuum) or shared with another component. Surfaces in optical contact are treated using Snell's law of refraction:

$$\frac{\sin(\theta'_i)}{\sin(\theta'_t)} = \frac{n_2}{n_1}$$

0-7803-8257-9/04/$20.00 © 2004 IEEE.

where n_1 and n_2 are respectively the refractive indices of the first and second media at an interface, and θ'_i and θ'_t are respectively the angles of incidence and transmission with respect to the surface normal.

B. Surface Definitions

If the "POLISH" surface finish is chosen, a reflection coefficient may also be specified to represent an external diffuse reflector. The value of the reflection coefficient determines the probability that a photon stays within the volume. Photons incident on the surface are assumed to have random polarization. If a change in refractive index occurs at the surface, the following probability calculation is made based upon Fresnel reflection [2]:

$$R = \frac{1}{2}\left[\frac{\sin^2(\theta'_i-\theta'_t)}{\sin^2(\theta'_i+\theta'_t)} + \frac{\tan^2(\theta'_i-\theta'_t)}{\tan^2(\theta'_i+\theta'_t)}\right],$$

where θ'_i and θ'_t are respectively the angles of incidence and transmission with respect to a local normal of the surface. If reflection is selected, the angle of reflection is set equal to the angle of incidence. If reflection does not occur, the photon is transmitted with the complementary probability T:

$$T = 1 - R,$$

where R was the previous probability based on Fresnel's equation, and the photon is assumed to obey Snell's law of refraction. Depending on the refractive index change and the angle of incidence, this may result in total internal reflection or refraction of the photon through the surface and into the adjacent component. If a reflection coefficient has been specified, the photon may be reflected back into the volume.

A "GROUND" surface finish can be specified in order to simulate a roughened or ground optical surface. It is treated in the same way as the polished surface described above, except that the normal to the surface used in the refraction calculations is randomly distributed, following a Lambertian distribution, around the nominal surface normal.

The "PAINT" surface finish models a surface painted with a diffuse reflecting material characterized by user-defined reflection coefficients. If random sampling shows that reflection occurs, it is assumed to be Lambertian. In this case, the angle of reflection is independent of the angle of incidence, and is sampled from a distribution given by

$$I(\theta) = I(0)\cos(\theta),$$

where $I(\theta)$ is the reflected intensity with respect to the surface normal and I(0) is the incident intensity.

The "DETECT" surface finish represents a photosensor (e.g. a photocathode or any other photon detecting layer of a photomultiplier tube). Unless otherwise specified, every photon reaching the photocathode is detected.

C. BUILDER Version 6.0

The BUILDER program simplifies the task of defining the geometrical properties of a model in DETECT by translating a higher level component definition syntax into the language of DETECT [2-5]. For example, the user can define sophisticated scintillation detector designs by connecting simple box components with a block scintillator. Once each component has been defined, BUILDER connects them, checks for overlaps and incompatible surface finishes, and then translates these higher level definitions into the language of DETECT2000.

III. Results and Discussion

We used DETECT2000 to determine the optimal crystal material and geometry, surface finishes, and coupling conditions for our Position Sensitive Photomultiplier Tube (PSPMT).

A. Optimizing Photon Output: Choosing LSO

In order to study light collection efficiency, we simulated point light sources at different depths within several crystal materials using the properties shown in Table I. The results are shown in Fig. 1.

Table 1. Relevant properties of scintillation crystals used in light tracking simulations.

Scintillator	Linear Attenuation Coefficient (cm^{-1})	Crystal Length for 93% Absorption 140 keV (mm)	Refractive Index	Approx. Light Yield 140 keV (photons)	Decay Time (ns)
NaI(Tl)	2.61	10.0	1.85	4200	230
CsI(Tl)	3.85	7.5	1.79	4200	1000
CsI(Na)	3.85	7.5	1.79	3150	650
LSO(Ce)	9.74	3.0	1.82	3150	40
BGO	12.15	2.4	2.15	630	300
GSO(Ce)	6.68	4.4	1.91	1050	60

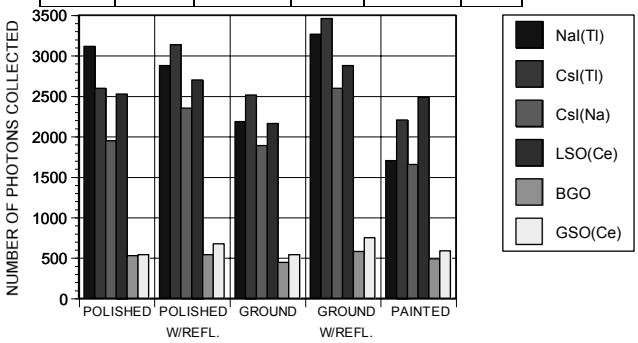

Figure 1. Absolute number of photons collected from 2 mm x 2 mm cross-section crystals of different lengths and surface conditions ("REFL:"=white reflector).

Note that although CsI(Tl) appears to collect the most photons, its emission peak wavelength is 580 nm, which is not a good spectral match to the absorption spectrum of a PMT photocathode, and will result in a significantly lower quantum efficiency [6]. The next highest absolute light collection is from NaI(Tl). However, this crystal material is hygroscopic, and thus requires a hermetically sealed package, which can be expensive, especially for crystal arrays [6]. The crystal material with the next highest light output into the PMT is LSO(Ce). A noteworthy feature of LSO(Ce) is that due to its high effective Z (66) and density ($7.4 g/cm^3$), just 3 mm thick LSO is required for 95% detection efficiency of 140 keV photons. A benefit of thin crystal dimensions is improved light

collection and narrow light spread. Fig. 2 below illustrates that because LSO can be thinner for the same stopping power as NaI(Tl), the light distribution is narrower in a sheet configuration, which will yield better intrinsic spatial resolution.

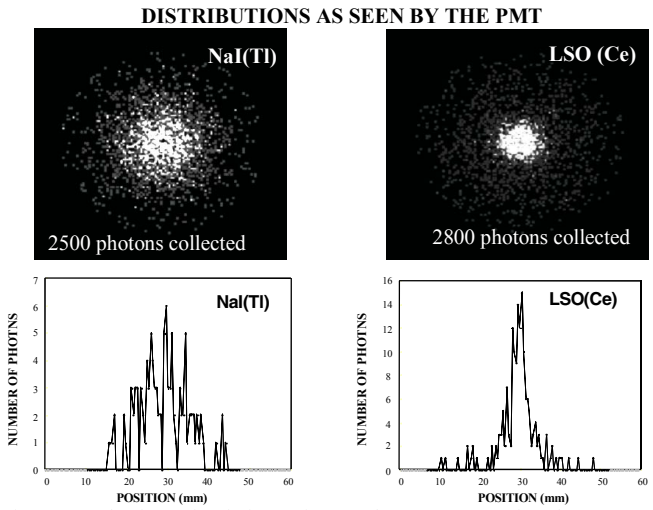

Fig. 2: Results from simulations of 5000 photons generated at the center of 5 cm x 5 cm crystal sheets. **Top Left**: NaI(Tl) sheet, 10 mm thick; **Top Right**: LSO(Ce) sheet, 3.5 mm thick. **Bottom**: Profiles through the distributions.

For these reasons, we concluded that LSO:Ce is the best choice for our gamma camera, even though NaI(Tl) has been the standard scintillation crystal for gamma cameras, and LSO is normally used in Positron Emission Tomography (PET) [1].

B. Measured ^{176}Lu Background Rate in LSO Array

We measured the ^{176}Lu background rate of LSO in order to determine whether or not it would be problematic for our purposes. Fig.3 shows approximately 2.6 million background events in a 23x23 array of 2 mm x 2 mm x 3 mm LSO crystals.

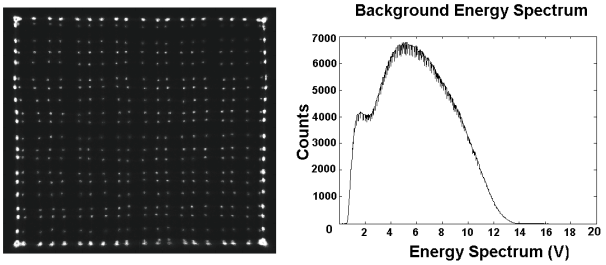

Fig. 3: **Left**: Background events for the LSO array. Multiple rows of crystals on the same anode row at PSPMT edges produces the hot perimeter artifact. **Right**: Energy spectrum shows well-known characteristics of a beta emitter.

The measured total background rate (room + ^{176}Lu) using an open energy window was ~63 cps/cm^3, or ~0.76 counts per second (cps) per crystal, which is low since the volume of each 2 mm x 2 mm x 3 mm LSO crystal is only 0.012 cm^3. With a narrow energy window centered at 140 keV, the background rate is negligible for most of the source activities we expect. We measured LSO background rates of approximately 1.6 cps/cm^3 in a 20% window about 122 keV, which for a 5 cm x 5 cm x 0.3 cm crystal volume translates into a background rate of only 12 cps over the 5 cm x 5 cm FOV or 0.02 cps per LSO crystal.

C. Light Distribution Linearity: Continuous Crystal versus Discrete Crystal Array

We initially investigated continuous crystals to evaluate light distribution linearities. Fig. 4 illustrates that for a 3.5 mm thick continuous LSO sheet, light collection efficiency is higher and the light distributions are narrower than for a 10 mm thick continuous NaI(Tl) sheet.

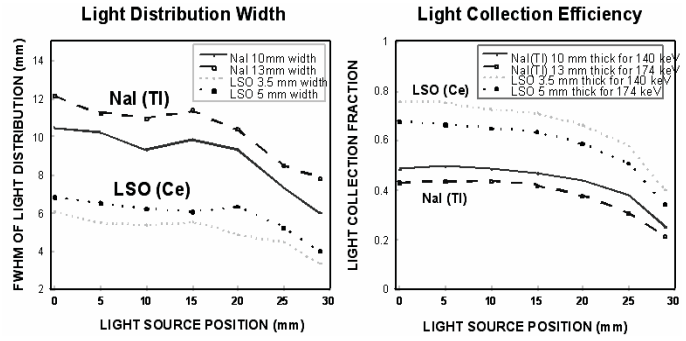

Fig. 4: **Left**: FWHM of the light distributions as a function of light source position for 10 and 13 mm thick NaI(Tl) and 3.5 and 5 mm thick LSO crystals (5 cm x 5 cm area, no entrance window). The different crystal thicknesses correspond to >95% absorption efficiency for 140 and 170 keV photons, respectively. Light distribution widths were extracted from fits to a Lorentzian distribution. **Right**: Fraction of light collected as a function of source position.

However, the light distribution non-linearities in crystal sheets seen in Fig. 4 above will be problematic for a small 5 cm x 5 cm FOV camera. As a result, we investigated light distribution linearity for an array of discrete crystals. Figure 5 plots the number of light photons collected as a function of position of a point source of 5000 light photons. All three figures represent simulations of 20 x 20 arrays of 2 mm x 2 mm x 3 mm LSO crystals, with 10 μm optical coupling grease between the array and PSPMT, and reflector on the perimeter and top of the array block.

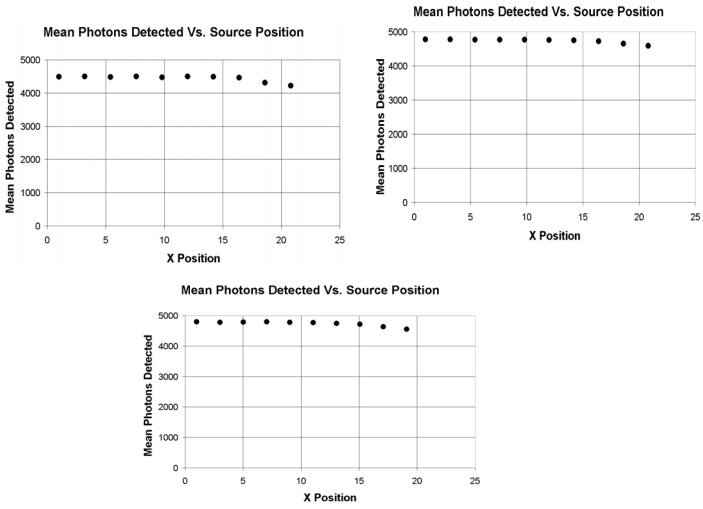

Fig: 5: Light collection vs. light source position (mm) from center to one edge. **Top Left**: Array of polished crystals with inter-crystal reflectors. **Top Right**: Array of ground crystals with inter-crystal reflectors. **Bottom**: Array of ground crystals without inter-crystal reflectors. For all figures, 5000 photons were simulated.

As seen in Fig. 5, simulations of these discrete crystal arrays exhibit improved light distribution linearity compared to continuous crystals (Fig. 4) independent of surface conditions and reflectors. This improvement is due to the isolation of the individual crystal pixels and resulting light focusing onto the photodetector.

D. Light Distribution Width for Crystal Array

We investigated the 20 x 20 crystal array light distribution width for various individual crystal surface treatments and crystal-PMT coupling, as shown in all subsequent simulations. All other array specifications are identical to those in the previous section.

Fig. 6 and 7 show light distributions as seen by the PSPMT for 5000 simulated light photons and their profiles for an array of ground crystals without and with inter-crystal reflector, respectively. Note that for each light distribution image, the three distributions shown were generated separately and then summed.

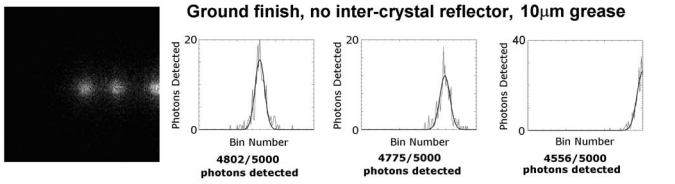

Fig. 6: These distributions correspond to moving a source across the face of a 20 x 20 array of ground LSO crystals with no inter-crystal reflector.

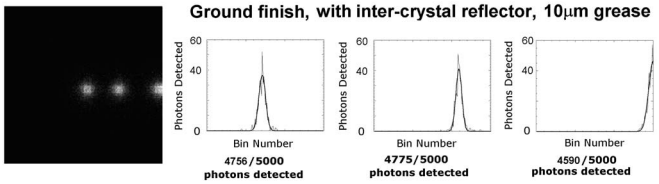

Fig. 7: These distributions correspond to moving a source across the face of a 20 x 20 array of ground LSO crystals with inter-crystal reflector.

Further studies using a more realistic grease thickness and different crystal features are shown in Fig. 8 and 9.

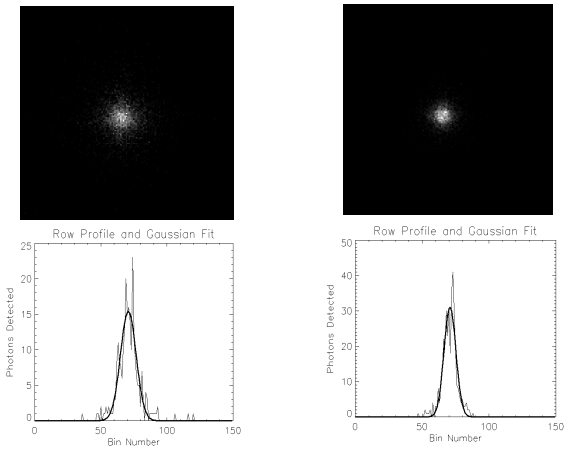

Fig. 8: **Left**: Ground crystals, no reflector, with thick (100 μ m) coupling grease. 4800/5000 photons **Right**: Ground, with reflector, with thick (100 μ m) grease. 4786/5000 photons.

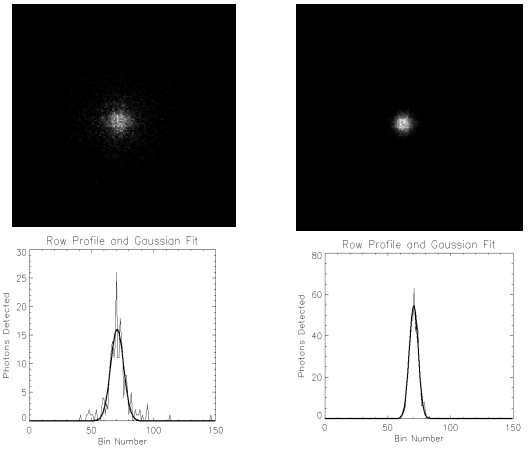

Fig. 9: **Left**: Ground crystals, no reflector, no grease. 4510/5000 photons. **Right**: Ground crystals, with reflector, no grease. 4518/5000photons.

Note that the conditions of no inter-crystal reflector and coupling grease between the array and PSPMT (Fig. 8 left) tend to increase light diffusion onto the PSPMT face, while the conditions of inter-crystal reflector and no grease (Fig. 9, right) tend to improve the light focusing onto the PSPMT. Thus, the overall narrowest light distribution case is when there is inter-crystal reflector and no coupling grease (Fig. 9, right). A narrow light distribution is desirable for high spatial resolution, however adequate light diffusion is necessary to spread the light among the 6 mm x 6 mm PSPMT anodes for uniform and linear positioning. It is interesting to note that the use of coupling grease for crystals with or without inter-crystal reflector (Fig. 8) tends to diffuse light to a greater extent than not using coupling grease with comparable overall light transmission into the PMT (Fig. 9).

Both the FWHM and FWTM for all of these simulations are summarized in Fig. 10.

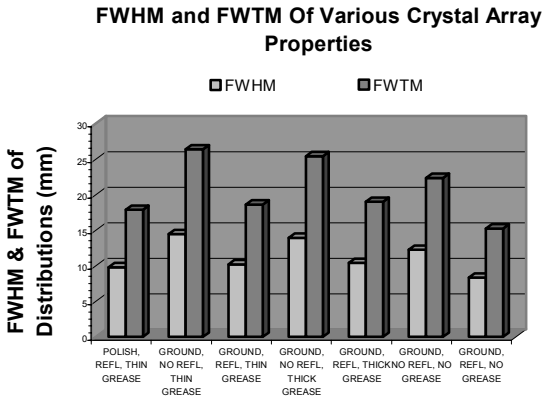

Fig. 10: FWHM and FWTM for all discrete crystal array simulations.

E. Experiments

Experiments were performed by flood irradiating a 5 x 5 array of 2 mm x 2 mm x 3 mm LSO(Ce) crystals with a ^{57}Co source (122keV). For all cases the outer array border was wrapped in Teflon tape. The setup utilized a charge multiplexed readout of a Hamamatsu H8500 PSPMT [7]. Each of the images shown in Fig. 10 represents ~262,000 counts.

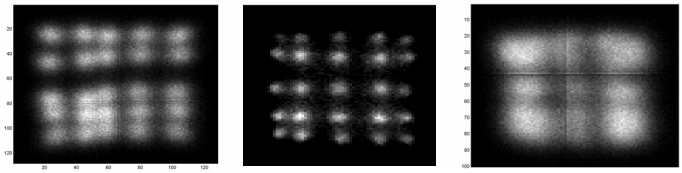

Fig. 11: **Left**: Ground, without reflector, without grease. **Middle**: Ground, with reflector, with thick grease. **Right**: Ground, without reflector, with thick grease

The crystal flood images are consistent with the simulation results of light distributions. The conditions of no inter-crystal reflector and no optical coupling grease (Fig. 11 Left) focus the light to some extent, but also tend to spread out the light, which explains why the crystals are not as well distinguished. The conditions of inter-crystal reflector and with coupling grease (Fig. 11 Middle) tend to sharpen the light distribution making the crystals better delineated, and with relatively poor light diffusion due to the inter-crystal reflectors. As seen in Fig. 11 (Right), the ground no reflector with grease exhibits over-diffusion of light.

IV. Summary and Conclusions

Our objectives in designing the scintillation crystal array for a miniature gamma ray camera include optimizing light collection, spatial linearity, and spatial resolution.

In comparison to other types of scintillation crystals, we chose LSO(Ce) because of its compatibility with the absorption spectrum of a PMT photocathode, its high stopping power at 140keV (just a 3 mm thickness is required), and its low cost compared to hermetically sealed NaI(Tl) arrays. Because of the low volume of LSO required, the background rate is low (~0.02 cps per 2 mm x 2 mm x 3 mm LSO crystal in a 20% window around 122 keV).

Spatial and spectral non-linearities in sheet crystals can be problematic for our small 5 cm x 5 cm FOV camera, since we want the entire FOV to be sensitive. Since an array of discrete crystals exhibits better spatial linearity, the camera response will be more uniform and linear towards the edge, which is especially important for a small FOV camera in the lymph node imaging application proposed.

Simulation studies have shown that the ground crystal finish, no inter-crystal reflector, with optical coupling grease conditions tend to spread the light more onto the PSPMT than do the ground, with reflector, non-greased crystal arrays. Although the latter conditions improve light focusing, more light diffusion may be necessary for adequately spreading light among the 6mm x 6mm PSPMT anodes for accurate positioning.

Experimental data from the ^{57}Co flood images are consistent with simulation results of light distributions. The conditions of no inter-crystal reflector and no coupling grease tend to focus, but also spread out the light, which explains why the crystals are not as well distinguished. The conditions of inter-crystal reflector and with coupling grease tend to sharpen the light distribution making the crystals better delineated; however, the light distribution image for this array exhibits poor light diffusion due to the inter-crystal reflectors.

V. Acknowledgements

This project has been supported in part by research grant RG-01-0492 from the Whitaker Foundation, and by the Howard Hughes Undergraduate Research Apprenticeship Program at the University of California, San Diego.

VI. References

[1] C. S. Levin, "Detector design issues for compact nuclear emission cameras dedicated to breast imaging," *Nuclear Instruments and Methods in Physics Research,* A 497, pp. 60-74, 2003.

[2] C. Moisan, F. Cayouet, and G. McDonald. DETECT2000: the object oriented C++ language version of DETECT: a program for modeling optical properties of scintillators. Department of Electrical and Computer Engineering at Laval University. Quebec City, Quebec, Canada. Available: http://www.gel.ulaval.ca/detect/

[3] C. Moisan and G. McDonald. BUILDER: a high level language interface to DETECT for the design of scintillation detectors: user's manual, version 6.0. Department of Electrical and Computer Engineering at Laval University. Quebec City, Quebec, Canada. Available: http://www.gel.ulaval.ca/detect/

[4] C. Moisan, F. Cayouet, and G. McDonald. (2000, September 1) DETECT2000, version 5.0. Available: http://www.gel.ulaval.ca/detect/

[5] C. Moisan and and G. McDonald. (2000, September) BUILDER Ver6.0. Available: http://www.gel.ulaval.ca/detect/

[6] C. S. Levin, E. J. Hoffman, M. PO. Tornai, and L. R. MacDonald, "PSPMT and photodiode designs of a small scintillation camera for imaging malignant breast tumors," *IEEE Trans. Nucl. Sci.,* vol. 44, no. 4, pp.1513-1520, Aug. 1997.

[7] P. D. Olcott, J. A. Talcott, C. S. Levin, F. Habte, and A. M. Foudray, "Compact readout electronics for hand-held gamma ray imagers," Presented at the 2003 IEEE Medical Imaging Conference. Abstract No. M3-157.